CO2 Impact Analysis for Road Embankment Construction: A Comparative Environmental Assessment of Lignin and Lime Soil Stabilization Treatments

Perri, Giusi; De Rose, Manuel; Domitrović, Josipa; Vaiana, Rosolino

Source / Izvornik: **Sustainability, 2023, 15**

Journal article, Published version
Rad u časopisu, Objavljena verzija rada (izdavačev PDF)

https://doi.org/10.3390/su15031912

sustainability

MDPI

Article

CO_2 Impact Analysis for Road Embankment Construction: Comparison of Lignin and Lime Soil Stabilization Treatments

Giusi Perri [1,*], Manuel De Rose [1], Josipa Domitrović [2] and Rosolino Vaiana [1]

[1] Department of Civil Engineering, University of Calabria, 87036 Rende, Italy
[2] Faculty of Civil Engineering, University of Zagreb, 10000 Zagreb, Croatia
* Correspondence: giusi.perri@unical.it

Abstract: The last decade has witnessed increased attention toward products, services, and works with reduced environmental impacts. In the field of road construction, the use of alternative materials, wastes, or by-products obtained from industries is attracting considerable interest. The Life Cycle Assessment (LCA) is a powerful project-level tool that allows the assessment of the environmental impacts of a road infrastructure, from raw materials production to end of life phase. In this study, the environmental impacts (in terms of global warming potential-GWP) of an embankment construction project are investigated by a cradle-to-gate approach. The analysis focuses on all the processes involved in the construction of an embankment section, from the base to the preparation of the pavement formation level. The results are provided for two different road types and two different stabilization methods, including the use of lignin and lime. All processes that contribute towards global warming are investigated and described in detail. The most important finding of the LCA, in terms of GWP, is that the production of materials is the phase that contributes the significant share of the total environmental impact (more than 90%) for all scenarios. The lowest production-related emissions can be recorded for the scenarios involving lignin treatment for the stabilization of the embankment body. Furthermore, the percentage increase in GWP ranges between 51% and 39% for transportation activities and 10–11% for construction activities, comparing the scenarios including lime stabilization with the scenarios involving lignin treatment.

Keywords: carbon footprint; soil stabilization; road construction; sustainable construction; waste reuse; life cycle assessment (LCA); alternative materials; environmental impacts; sustainability

Citation: Perri, G.; De Rose, M.; Domitrović, J.; Vaiana, R. CO_2 Impact Analysis for Road Embankment Construction: Comparison of Lignin and Lime Soil Stabilization Treatments. *Sustainability* **2023**, *15*, 1912. https://doi.org/10.3390/su15031912

Academic Editor: Antonio Caggiano

Received: 31 December 2022
Revised: 13 January 2023
Accepted: 16 January 2023
Published: 19 January 2023

1. Introduction

Transport infrastructures play a fundamental role in connecting different districts and countries, contributing to the social, cultural, and economic growth of large areas [1]. In such a context, roads have a strategic significance, as they account for the largest proportion of transport in the EU (European Union) [2].

As kilometers of roads are being constructed worldwide and since this number is expected to grow, the pavement engineering industry needs to perform a smooth transition to a more sustainable and circular way of operating [3,4]. In fact, transportation infrastructures, and road pavements in particular, contribute not only to significant public administration expenditure but also to energy and water consumption, the depletion of natural resources, and the emission of greenhouse gases (GHGs) [5].

In 2016, the European Commission published the document "Green Public Procurement Criteria for Road Design, Construction and Maintenance" [6], in order to encourage the purchasing of products, services and works with reduced environmental impacts; moreover, at the end of 2019, it adopted the European Green Deal [7], in order to meet the target of zero GHG emission by 2050.

Therefore, with the aim of pursuing these goals, decision-makers and researchers have been focused on developing different methodologies to assess sustainability, also in the field of road construction [8]. A widely accepted and standardised method (ISO 14040-series) for quantifying and assessing the potential environmental impacts of road pavement is the Life Cycle Assessment (LCA) [9], which helps to quantify, analyze, and compare the environmental impacts of different types of pavement from material extraction to their end of life [10].

Several LCA applications have dealt with road infrastructures and, in particular, with the analysis of the road pavement [11–13]; however, very few applications are applied for the construction of embankments or road subgrades [14–16]. Moreover, due to the increasing interest in the use of alternative materials, wastes, or secondary raw materials in road construction works [17], the LCA becomes a powerful and useful tool in assessing the potential environmental benefits that could be achieved in comparison with the current state of the practice (current state of knowledge) [18].

In addition, among the different recycled materials investigated in the road industry, lignin is gaining more and more popularity as a sustainable reuse option for several applications in civil engineering work [19,20]. In fact, lignin is the most common and widespread biopolymer on Earth; moreover, as paper industries and biorefineries produce millions of tons worldwide every year, it is broadly available [21].

The last decade has witnessed a plethora of useful and promising applications for lignin, including as a bitumen extender [22], as a partial replacement in bituminous binders [23], or as fibers in asphalt mixtures [24].

Another encouraging example is the application of lignin as an environmentally friendly stabilizing agent of rejected or marginal existing in-situ soils, whose good mechanical properties are confirmed in different laboratory and field investigations [20,25,26]. Based on these results, an effort should be made to assess the environmental viability of using lignin-stabilized soil in road embankments.

Therefore, this study addresses this need through a comparative LCA analysis for a typical high-volume traffic Italian road embankment. In particular, a more common quicklime soil stabilization and a lignin stabilization were compared; moreover, two different roads were selected for the analysis: a highway and a secondary rural road, for a total of four different scenarios.

For each defined scenario, the pavement structure was designed in order to meet the standard structural requirements, depending on the materials used. The LCA analysis quantitatively assessed the environmental impacts during the materials' production, transportation, and construction phases, with a cradle-to-gate approach.

2. Materials and Methods

Part 2 of this paper outlines the assumptions and methods implemented in the study. The general structure of this section is organized as follows: Section 2.1 (goal and scope definition) and Section 2.2 (system boundaries and functional unit) present two significant elements of the LCA framework, according to the related standards; Section 2.3 provides detailed assumptions on the soil stabilization (Section 2.3.1), on the methodology used in GHG assessment (Section 2.3.2), and on the evaluation of the impacts related to transportation (Section 2.3.3) and construction (Section 2.3.4) activities. Sections 2.4 and 2.5 explore and detail the activities and processes related to each life-cycle stage (production, transportation, and construction).

2.1. Goal and Scope Definition

This study provides the results of an LCA of an embankment construction project on a 1-km-long section of two Italian roads. The roads selected can be classified as a highway, an A class road and a secondary rural road, a C1 class road, in accordance with the Italian standard D.M. 5/11/01 "Functional and Geometric Standards for Road Construction" [27].

Furthermore, two different stabilization methods were investigated, including the use of lignin and lime. Stabilization allows the minimization of the environmental impacts and contributes to the decrease in project costs, as it is an effective treatment for re-using in-situ soil [28,29].

The environmental impacts involved in the lifecycle phases of the embankment construction were assessed in terms of global warming potential (GWP), with a 100-year time horizon. The main purpose of the analysis was to evaluate the environmental impacts in terms of carbon footprint (amount of CO_2 emissions associated with the specific activities), related to the stabilization of soil with lime and lignin.

2.2. System Boundaries and Functional Unit

The functional unit (FU) used in this study was 1 km of road embankment. The analysis includes all the processes involved in the construction of an embankment section from the base to the preparation of the pavement formation level.

The total depth of the embankment was 2 m for both road sections. The width changed depending upon the considered road: the width of the highway was 14.50 m, the width of the rural road was 11.50 m.

For comparison purposes, the impacts were related to a unit of service, which was 1 m^3 of the road embankment section.

The analysis was developed from cradle to gate, focusing on the construction phase; it also included material extraction and production, and the transportation of materials. Drainages and erosion measures were not included in the analysis.

2.3. General Assumptions

2.3.1. Soil Stabilization

For the embankment body and subgrade construction, it was assumed that locally available soil deposits were used (e.g., the soil volume obtained from the excavations of cut sections within the site). This assumption allowed the elimination of the costs related to the option of using a better quality of borrow soil [30]. The replacement of locally weak soils with a higher quality of soil also increased the time of the operations and the environmental impacts related to the production of the aggregates and the waste from excavated soil. However, in-situ soil does not always meet the construction standards.

The in-situ soil properties are summarized in Table 1.

Table 1. Properties of in-situ soil.

Property	Characteristic
Particle Size Distribution [%]	
Gravel (2–75 mm)	28.2
Coarse sand (0.425–2 mm)	13.1
Fine sand (0.075–0.425 mm)	8.4
Silt and clay (<0.075 mm)	50.3
Atterberg Limits [%]	
Liquid Limit (LL)	38
Plasticity Limit (PL)	20
Plasticity Index (PI)	18
Standard Proctor compaction test	
Optimum water content (w_{opt}) [%]	13.4
Maximum dry unit weight ($\gamma_{d,max}$) [kg/m^3]	1910
Modified Proctor compaction test	
Optimum water content (w_{opt}) [%]	10.3
Maximum dry unit weight ($\gamma_{d,max}$) [kg/m^3]	2038
AASHTO soil classification	A-6

Given the significant presence of the clay matrix (about 50%), the soil had a poor performance to be reused as fill without preliminary treatment. Two stabilizing agents were used to upgrade the properties of the clayey soil: lime, which use is widespread in road stabilization, and lignin, a waste product (obtained from paper and pulp industry) that has also recently been used as a soil stabilizer.

Several laboratory tests were carried out to investigate the stabilized soil behavior in different conditions, to choose the appropriate treatment formulations, and to assess the corresponding performance-related properties. In particular, in the experimental plan, both the untreated and stabilized soils were characterized by physical and mechanical tests, such as Atterberg limits, CBR (California Bearing Ratio), UCS (Unconfined Compressive Strength), and ITS (Indirect Tensile Strength) tests. All methods and results are reported in a previously published study [25]. The optimum content of lignin and lime was 0.4% (as a percentage of the optimum water content) and 2.5% (as a percentage of soil dry weight), respectively.

In particular, the obtained results showed that the use of lignin as a stabilizing agent is appropriate for the treatment of the soil for the embankment body construction, but that it is unsuitable for subgrade construction. For subgrades, the standards [31] report that CBR values collected after wet conditioning (4 days) must range between 20 and 25%. As obtained in [25], lignin has a poor ability in upgrading the bearing capacity of the investigated soil in wet conditions (CBR value obtained for specimens immersed in a water bath for 4 days was 3.4%), whereas the 2.5% lime-treated soil allows us to record a CBR value of 22.5% in the same conditioning conditions. For this reason, in this study, the proper technique for stabilizing the pavement subgrade exclusively involved the use of lime for both scenarios. The applications investigated are summarized in Figure 1.

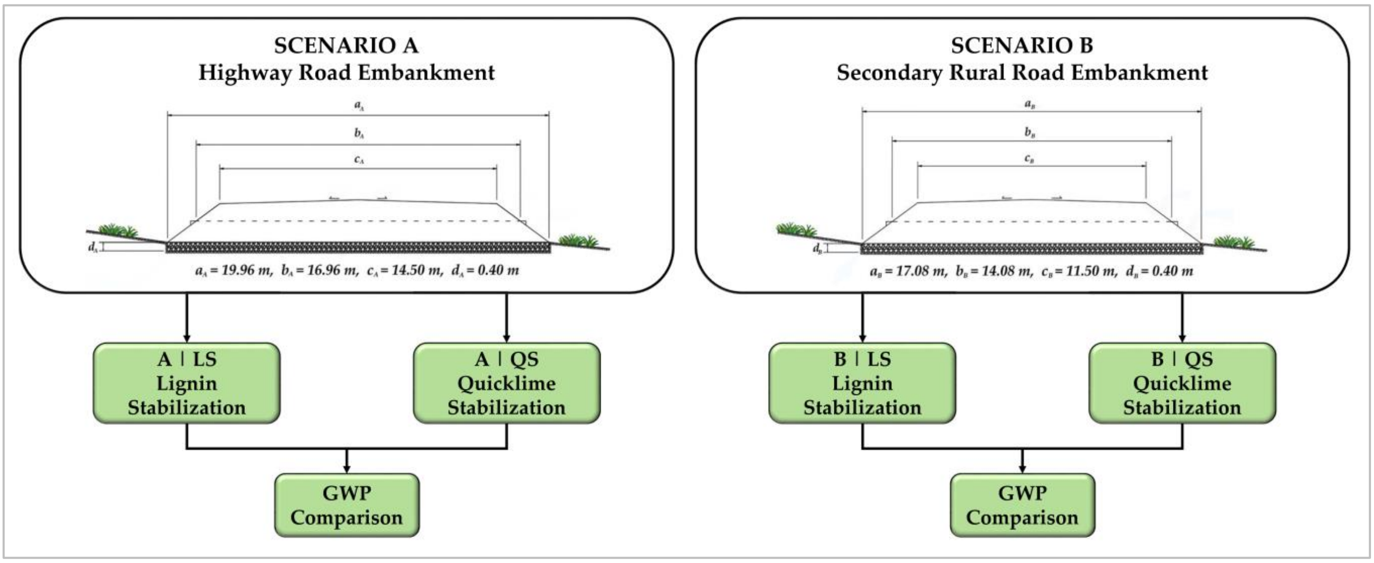

Figure 1. Summary of the LCA application.

The selection of the two types of roads was strictly related to the fact that the standards require specified structural quality criteria for the subgrade and embankment layers, which are different for each road type. In particular, the following acceptance thresholds are required [31]:

For the embankment body,

- highway: $\gamma_{d,max} \geq 92\%$ of the maximum dry unit weight obtained by the laboratory modified Proctor compaction test;
- secondary rural road: $\gamma_{d,max} \geq 97\%$ of the maximum dry unit weight obtained by the laboratory standard Proctor compaction test.

Then, for the subgrade,

- highway: $\gamma_{d,max} \geq 95\%$ of the maximum dry unit weight obtained by the laboratory modified Proctor compaction test;
- secondary rural road: $\gamma_{d,max} \geq 100\%$ of the maximum dry unit weight obtained by the laboratory standard Proctor compaction test.

Given these design specifications, the expected maximum dry density values for the lignin-treated soil and the lime-treated soil are shown in Table 2. In order to achieve the optimal compaction level, field compaction values must be as close as possible to these values obtained by laboratory tests.

Table 2. Maximum dry unit weight and optimum water content for each scenario.

Application	$\gamma_{d,max}$ [kg/m^3]	w_{opt} [%]
Scenario A | LS	2038	10.33
Scenario A | QS	1956	11.69
Scenario B | LS	1910	13.40
Scenario B | QS	1820	15.20

During construction operations, the A-6 soil is transported to the construction site and then embanked, treated, and compacted. It was assumed that a soil expansion of about 19% would be taken into account for the difference between the loose soil volume that is excavated and transported, and the soil volume in the embankment after compaction.

2.3.2. Assessment of Greenhouse Gas Emissions

In the LCA procedure, the data collected in the phase of Life Cycle Impact (LCI) were assigned to impact categories during the Life Cycle Impact Assessment (LCIA) analysis. In this study, the impact category investigated was global warming potential (or climate change). All the significant environmental processes contributing towards global warming were analyzed individually; then, all different flows were aggregated, expressing the GWP impact in terms of kg of carbon dioxide equivalents (kg CO_2-eq). This common unit was used to compare the emissions of different GHGs that contribute toward GWP in a different way; this is because each gas has different radiative properties and lifetime in the atmosphere [32]. The GHGs assessed in this work were carbon dioxide (CO_2), nitrous oxide (N_2O), and methane (CH_4). The CO_2-eq was obtained by summing the CO_2-eq of each gas, which was given by the product between the emission of a GHG and its global warming potential for a time horizon of 100 years. The GWP values are reported by the Environmental Protection Agency (EPA) [33]; in more detail, the GWP value used for converting N_2O to CO_2 is 298, and when converting CH_4 to CO_2, a GWP value of 25 is assumed.

This study explores the environmental burdens associated with material production, construction, and transportation.

In the phases of construction and transportation, emissions are strictly attributable to fuel consumption; thus, the starting point of the assessment of GHG emissions is the calculation of the fuel needed for each task. GHG emissions were obtained by multiplying the fuel consumed in each activity by vehicles and earthwork machines with the emission factor. It was assumed that the emission factor for diesel was 2.60 kg of CO_2 per liter [34]. Emission factors for N_2O and CH_4 are reported in Table 3, depending on the vehicle type.

Table 3. Emission Factors for on-road and non-road vehicles [35].

Vehicle Type	CH_4	N_2O
	kg/L	kg/L
Construction/Mining Equipment	2.48×10^{-4}	2.30×10^{-4}
Industrial/Commercial Equipment	2.46×10^{-4}	2.30×10^{-4}
	kg/km	kg/km
Light-Duty Trucks	1.80×10^{-5}	1.33×10^{-5}

2.3.3. Assessment of Emissions Generated by Transportation Activities

Air emissions associated with fuel consumption during transportation activities can be obtained with the general equation:

$$\mathrm{Emission}_{ij} = \mathrm{FC}_{(transport-v)j} \times \mathrm{EF}_i \tag{1}$$

where FC is the fuel consumption of the specific vehicle "v", and the subscripts "i" and "j" stand for the air pollutant and the transport activity, respectively.

Aggregates for the coarse-grained layer were transported from the plant to the construction site by 32 t trucks [36]. This type of vehicle was also considered to be used for local soil movement and quicklime transportation from the source to the worksite.

Fuel consumption $\mathrm{FC}_{\text{transport-truck}}$ [L/m^3] for the selected truck was computed as follows [37,38]:

$$\mathrm{FC}_{transport-truck} = \frac{K \times d \times I_c}{C} \tag{2}$$

where K is a coefficient related to the difference in fuel consumption between a full-loaded truck and an empty one (K = 1.7),

d [km] is the mean distance travelled during the transport-related activity,

I_c [L/km] is the fuel consumption at maximum load of the specific truck,

C [m^3] is the truck capacity.

Tanker trucks were used to transport water and lignin from sources to the worksite. The fuel consumed in the transport of these materials was calculated on the basis of the total number of trips NT (trips include empty returns); more specifically, the number of trips needed was obtained by dividing the volume to be transported by the tanker truck capacity (11,924 L/tank [39]). The fuel consumption associated with the tanker truck considered in this study $\mathrm{FC}_{\text{tankertruck}}$ was assumed to be 0.42 L/km [39], hence, the total fuel $\mathrm{FC}_{\text{transport-tankertruck}}$ can be calculated as follows:

$$\mathrm{FC}_{transport-tan\,kertruck} = \mathrm{FC}_{tan\,kertruck} \times d \times NT \tag{3}$$

where d (km) is the mean distance travelled during a single trip.

Emissions due to the transport of geotextile membranes by a small lorry with a payload of up to 3.3 t were assessed in the following way:

- CO_2 emissions [kg] were evaluated on the basis of the data available in the European Reference Life Cycle Database (ELCD) [40], and as a function of the distance covered [km] and the transported mass [t] by the truck.
- CH_4 [kg] and N_2O [kg] emissions were obtained by the product between the distance travelled [km] and the relative emission factor values reported by the EPA [35] for light trucks (Table 3).

The transportation distances for each material used in this study are shown in Table 4. An average distance of 1.2 km was considered for the transportation of in-situ soil (transport of the local soil to be treated from the temporary storage site to the worksite). Furthermore, the same distance was considered for transporting both lime and lignin to the worksite.

Table 4. Average transportation distances.

Input Materials	Transportation Distance [km]
Aggregates for the coarse-grained layer	20
Water	19
Geotextiles	55
Quicklime	30
Lignin	30

2.3.4. Assessment of Emissions Generated by Earthwork Machines

The assessment of the greenhouse gas emission "i" generated in the activity "j" by earthwork machines follows the general function:

$$\text{Emission}_{ij} = \text{FC}_{(eq-m)j} \times \text{EF}_i \tag{4}$$

where FC indicates the fuel consumption of the specific machine "m" and EF is the emission factor (Table 3).

The general function for the assessment of the fuel consumption (1 m^3 of activity) of the vibratory roller $FC_{eq\text{-}roll}$ [L/m^3] and the excavator $FC_{eq\text{-}exc}$ [L/m^3] is the following [37,41]:

$$\text{FC}_{eq-(\text{roll or exc})} = \text{P} \times \text{SC} \times \frac{\text{LF}_1 + \text{LF}_2}{2} \times \frac{1}{\rho_{fuel}} \times \text{Pr} \tag{5}$$

where P [kW], SC [kg/kWh], and Pr [h/m^3] are the power, the engine specific consumption, and the productivity of the equipment, respectively. The SC at full power ranges between 0.213 kg/kWh and 0.268 kg/kWh [41]; an average value of 0.25 kg/kWh is assigned to this parameter, as suggested by the existing literature [37]. ρ_{fuel} is the mean specific weight of the fuel, which is assumed to be 0.85 kg/L [41].

LF_1 and LF_2 are engine load factors, depending on the equipment type. As illustrated by [37], load factors can be assessed by specific laws, as follows:

- For the vibratory soil compactor

$$\text{LF}_1 = 0.05173e^{0.00142D} \tag{6}$$

$$\text{LF}_2 = 0.21032G^{0.43210} \tag{7}$$

- For the excavator

$$\text{LF}_1 = 0.0339e^{0.0014D} \tag{8}$$

$$\text{LF}_2 = 0.2007e^{0.0262t} \tag{9}$$

where D [kg/m^3], G [%], and t[min] are the material density, the grade of the slope, and the duration of use, respectively.

The productivity of the excavator is assumed to be 400 m^3/h [42]. The productivity for the vibratory soil compactor Pr_{roll} [m^3/h] can be calculated using the following equation [43,44]:

$$\text{Pr}_{roll} = (\text{L} \times \text{V} \times \text{S})/\text{N} \tag{10}$$

where L [m] is the compacted width per pass, V is the average speed in kilometers per hour, S is the compacted thickness, in millimeters, and N is the number of machine passes to achieve the desired compaction. Equation (11) gives the number of passes of the roller in order to achieve compaction, as a function of the field dry density $\gamma_{d,field}$ [g/cm^3] and the moisture content w [%] [45]:

$$\gamma_{d,field} = 1.065 + 0.033 \times \text{w} + 0.084 \times \text{N} \tag{11}$$

Fuel consumed by the dozer $FC_{eq\text{-}doz}$, the binding agent spreader FC_{bas}, the soil stabilizer FC_{st}, and the motor grader FC_{mtg} is defined by:

$$\text{FC}_{eq-(\text{doz, bas, st or mtg})} = \text{FC} \times \text{ot}_{tot} \tag{12}$$

where FC [L/h] is the specific fuel consumption of the machine and ot_{tot} [h] is the total operating time required to complete the single activity. For example, for dozer activity, ot_{tot} is obtained from the relationship between the total volume of loose soil excavated by the dozer [m^3] and the dozer productivity Pr [m^3/h]. Information regarding the FC and Pr was collected from the manufacturer's specifications and previous studies [42].

2.4. Production of Input Materials

Life cycle inventory data was collected from the literature for the production of the materials. The contribution to the environmental lifecycle impacts is summarized in Table 5 for each input material.

Table 5. Average kg CO_2-eq emissions generated from each material production.

Process Code	Material	kg CO_2-eq/kg	Reference
PA	Aggregates for the coarse-grained layer	6.18×10^{-3}	[46]
PG	Geotextiles	2.35	[47]
PQ	Lime	0.94	[48]
PL	Lignin	0.26	[49]

2.5. Transportation and Construction Activities

All processes that contribute towards global warming are described and assessed in detail. The construction stages accounted for in this study are reported in Figure 2. Moreover, Figure 2 provides an overview of the construction and transportation operations that are considered for each scenario.

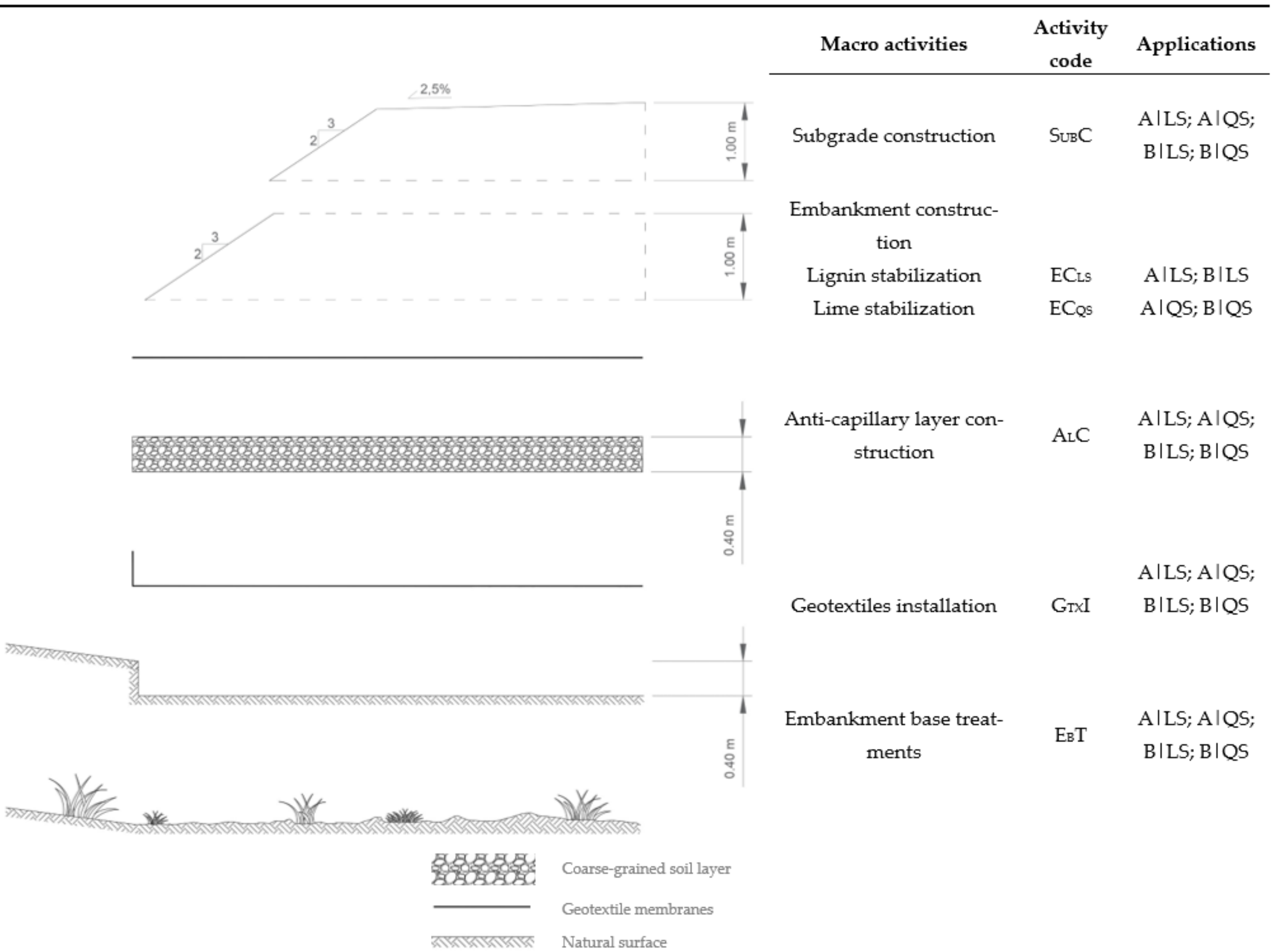

Figure 2. Construction stages.

The construction stage is divided into five subphases, which are discussed in the following sections.

2.5.1. Embankment Base Treatments (E_BT)

This phase included preliminary operations aimed at the preparation of the embankment base (E_BT | C). Surface vegetation and organic soil were removed to a depth of 30 cm below the ground level. This soil was not suitable to be used as fill embankment soil as it was high in organic material content. For this reason, it was temporarily stockpiled on the sides of the worksite as it was used for covering the finished embankment and restoring the local vegetation at the end of the works.

E_BT also includes the excavation of the soil for the construction of the anti-capillary layer (E_BT | E). In this case, the excavated material (A-6 soil) (plus the soil from the initial excavation) was used to fill up the embankment body. Trucks transported this soil to a temporary storage site (E_BT | T). All processes and equipment at this stage are listed in Table 6.

Table 6. E_BT: processes and equipment.

Activity Code	Input Resources	Process Code	Processes	Transport/ Construction Site Equipment	Output
E_BT	Fuel	E_BT | C	Cleaning and removing topsoil	Dozer	Emissions Embankment base
		E_BT | E	Excavation for the anti-capillary layer	Excavator	
		E_BT | T	Transport of the excavated soil to the temporary storage site	Truck (32 t)	

Table 7 provides the values of the engineered earth volumes in this phase.

Table 7. E_BT: engineered earth volumes.

	Process Code	Scenario A	Scenario B
Removed topsoil [m^3]	E_BT | C	6138.00	5274.00
Excavated soil [m^3]	E_BT | E	7984.00	6832.00
Transported soil to the temporary storage site [m^3]	E_BT | T	9902.23	8473.45

2.5.2. Anti-Capillary Layer Construction

The embankment design includes the construction of a granular layer with a capillary-breaking effect. The processes involved in this phase are reported in Table 8.

Table 8. A_LC: processes and equipment.

Activity Code	Input Resources	Process Code	Processes	Transport/Construction Site Equipment	Output
A_LC	Aggregates Water Fuel	A_LC | T_a	Transport of aggregates to the construction site	Truck (32 t)	Emissions Anti-capillary layer
		A_LC | T_w	Transport of water to the construction site	Tanker truck	
		A_LC | C	Compaction of the anti-capillary layer	Vibratory soil compactor	

Aggregates for the coarse-grained layer were transported from the quarry site to the construction area ($A_L C | T_a$). The soil used can be classified as A-3 (fine sand), according to the AASHTO soil classification [50].

A standard Proctor compaction test was carried out on this soil to define the maximum dry unit weight and the optimum water content; the values obtained for these parameters by the laboratory test were the following: $\gamma_{d,max}$ = 2290 kg/m^3 and w_{opt} = 6.02 % [25]. This analysis is required to assess the number of passes and the productivity of the roller. The values obtained by applying Equations (6), (7), (10) and (11) are summarized in Table 9.

Table 9. Main parameters for vibratory toller compactor fuel consumption assessment.

Characteristic	Value
N [-]	12
S [mm]	400
Pr_{roll} [m^3/h]	355
D [kg/m^3]	2020
G [%]	0
LF_1	0.91
LF_2	0

The hypotheses regarding the density of loose soil D are based on the values of previous studies [37]; in particular, a 10% soil expansion value was assumed in order to consider the difference between the loose soil volume and the soil density in the bank after compaction. The volume of aggregates required in Scenario A and Scenario B is 9051.17 m^3 and 7745.19 m^3, respectively.

The assumption was that, before compaction, additional water was provided to correct the soil moisture content. More specifically, it was supposed that the original water content was 2%, thus 4.02% more water was added to the treated soil. This last operation involves water transport to the worksite ($A_L C | T_w$).

2.5.3. Geotextiles Transport to the Construction Site and Installation

Geotextiles are used to protect the anti-capillary layer from the uncontrolled passage of soil particles, due to their filtering and separation functions. In addition, the installation of geotextiles is required to prevent intermixing between the granular soil and the underlying soil, preserving the drainage capacity and the structural integrity of the coarse-grained soil layer [51]. The geotextiles used in this study were 6.50 m wide with a mass per unit area of 255 g/m^2. The geotextiles were installed below the anti-capillary layer and at the interface between the anti-capillary layer and the embankment soil.

The geotextile installation-related operations are reported in Table 10. This construction step included two main activities: the transport of the geotextiles by a small lorry ($G_{TX}I | T$) and rolls handling by a forklift, supporting the laying operations ($G_{TX}I | L$). The emissions of the diesel forklift were obtained by an average of values from previous studies, considering drive with load and no load, and an average distance of 1.5 km [52].

Table 10. $G_{TX}I$: processes and equipment.

Activity Code	Input Resources	Process Code	Processes	Transport/Construction Site Equipment	Output
$G_{TX}I$	Geotextiles Fuel	$G_{TX}I | T$	Geotextiles transport to the construction site	Small lorry (3.3 t)	Emissions Geotextiles installed
		$G_{TX}I | L$	Geotextiles handling and installation	Forklift	

2.5.4. Embankment Body Construction: Lignin Stabilization

All the activities and each piece of equipment involved in this construction phase are shown in Table 11.

Table 11. EC_{LS}: processes and equipment.

Activity Code	Input Resources	Process Code	Processes	Transport/Construction Site Equipment	Output
EC_{LS}	Lignin Water Fuel	$EC_{LS}\,\vert\,T_s$	Transport of the A-6 soil	Truck (32 t)	Emissions Embankment body
		$EC_{LS}\,\vert\,T_L$	Transport of lignin to the construction site	Tanker truck	
		$EC_{LS}\,\vert\,T_w$	Transport of water to the construction site	Tanker truck	
		$EC_{LS}\,\vert\,SM$	Spreading and mixing	Soil stabilizer	
		$EC_{LS}\,\vert\,C$	Compaction of the layer	Vibratory soil compactor	

The first sub-process of the embankment body construction was the transport of the required volume of the A-6 soil from the stockpile sites to the construction area ($EC_{LS}\,|\,T_s$). The soil treatment by lignin also involves the transport of lignin ($EC_{LS}\,|\,T_L$) and water ($EC_{LS}\,|\,T_w$). The lignin used in this study was a dark brown liquid in a concentrated condition that required dilution before mixing (part of the required optimum water content was used) [25]. The optimum moisture content, as determined by the laboratory compaction test (standard or modified, depending on the Scenario, see Table 2), was used as a guide in the assessment of the proper moisture content, given that the original water content of the soil was 6%.

The volumes of soil and lignin needed for each scenario are provided in Table 12.

Table 12. Volumes of soil and lignin needed for each scenario.

	Process Code	Scenario A ǀ LS	Scenario B ǀ LS
Transported A-6 soil [m^3]	$EC_{LS}\,\vert\,T_s$	24,431.81	19,323.25
Imported lignin [t]	$EC_{LS}\,\vert\,T_L$	15.54	15.95

The placing, treatment, and compaction of fill material were carried out in two layers; the thickness of each layer was 50 cm and the working depth of the used soil stabilizer was 51 cm (Wirtgen WR 240 i). The soil stabilizer machine allowed the spread and mixing of the lignin and water into the existing soil. Each layer was uniformly compacted to the desired design specifications before the next layer was applied. Parameters for the assessment of the compaction sub-phase are reported in Table 13.

Table 13. Main parameters for compaction operations based on lignin stabilized scenarios.

Characteristic	Value	
	Scenario A ǀ LS	Scenario B ǀ LS
N [-]	7	4
S [mm]	500	500
Pr_{roll} [m^3/h]	760.71	1331.25
D [kg/m^3]	1540.00	1540.00
G [%]	0	0
LF_1	0.46	0.46
LF_2	0	0

2.5.5. Embankment Body Construction: Lime Stabilization

The same A-6 soil was treated by lime in the Scenario A ǀ QS and Scenario B ǀ QS. The sub-processes and transport/construction equipment are detailed in Table 14.

Table 14. EC_{QS}: processes and equipment.

Activity Code	Input Resources	Process Code	Processes	Transport/Construction Site Equipment	Output
EC_{QS}	Quicklime Water Fuel	$EC_{QS} \mid T_s$	Transport of the A-6 soil	Truck (32 t)	Emissions Embankment body
		$EC_{QS} \mid T_Q$	Transport of lime to the construction site	Tanker truck	
		$EC_{QS} \mid T_w$	Transport of water to the construction site	Tanker truck	
		$EC_{QS} \mid S$	Lime spreading	Binding agent spreader	
		$EC_{QS} \mid M$	Mixing	Soil stabilizer	
		$EC_{QS} \mid C$	Compaction of the layer	Vibratory soil compactor	

The addition of lime to A-6 soil increases the optimum moisture content and reduces the maximum dry density.

Table 15 reports the volume of soil to be transported for the construction of 1-km-long section and the quantity of lime required for the soil treatment, according to the design specifications, for both scenarios.

Table 15. Volumes of soil and lime needed for each scenario.

	Process Code	Scenario A	Scenario B
Transported A-6 soil [m^3]	$EC_{QS} \mid T_s$	23,451.15	18,412.73
Imported lime [t]	$EC_{QS} \mid T_Q$	903.00	709.00

The sub-process $EC_{QS} \mid S$ (Lime spreading) involves the use of the binding agent spreader (Wirtgen SW 16 MC). Soil treatment, mixing, and compaction are carried out for two layers 50 cm deep, as for the embankment stabilized by lignin. The compaction step-related parameters are summarized in Table 16.

Table 16. Main parameters for compaction operations based on lime stabilized scenarios.

Characteristic	Value	
	Scenario A | QS	Scenario B | QS
N [-]	6	3
S [mm]	500	500
Pr_{roll} [m^3/h]	887.50	1775.00
D [kg/m^3]	1540.00	1540.00
G [%]	0	0
LF_1	0.46	0.46
LF_2	0	0

2.5.6. Subgrade Construction and Preparation of Pavement Formation Level

Subgrade lime stabilization was required for each scenario as the in-situ soil was unsuitable for providing adequate support for pavement structure functionality during its service life, and lignin treatment does not fulfil the construction standards. The sub-processes involved in this phase (Table 17) were the same as the processes discussed for the embankment body construction (lime stabilization).

Table 17. $S_{UB}C$: processes and equipment.

Activity Code	Input Resources	Process Code	Processes	Transport/Construction Site Equipment	Output
$S_{UB}C$	Quicklime Water Fuel	$S_{UB}C \mid T_s$	Transport of the A-6 soil	Truck (32 t)	Emissions Subgrade and pavement formation level
		$S_{UB}C \mid T_Q$	Transport of lime to the construction site	Truck (32 t)	
		$S_{UB}C \mid T_w$	Transport of water to the construction site	Tanker truck	
		$S_{UB}C \mid S$	Lime spreading	Binding agent spreader	
		$S_{UB}C \mid M$	Mixing	Soil stabilizer	
		$S_{UB}C \mid C$	Compaction of the layer	Vibratory soil compactor	
		$S_{UB}C \mid F$	Precision-finishing	Motor grader Vibratory soil compactor	

Table 18 provides the values of the engineered soil volumes in each sub-phase and the quantity of lime required for the soil treatment of the 1-km-long sections.

Table 18. Soil volumes (transported and engineered) and lime quantities required in Subgrade construction.

	Process Code	Scenario A	Scenario B
Transported A-3 soil [m^3]	$S_{UB}C \mid T_s$	18,039.35	13,969.09
Imported lime [t]	$S_{UB}C \mid T_Q$	695.00	536.00
Engineered soil volumes during the precision-finishing phase [m^3]	$S_{UB}C \mid F$	3300	2700

Parameters involved in the assessment of fuel consumption during the compaction phase are the same as Table 16, except for LF_2, which is calculated taking into account the grade of the slope, of 2.5% ($LF_2 = 0.04$).

In addition, this last construction phase includes the preparation of the pavement formation level, slopes finishing, and the trimming of surfaces ($S_{UB}C \mid F$). The slopes of the finished embankments were covered with the topsoil stockpiled during the process and $E_BT \mid C$ for the re-establishment of site vegetation.

3. Results and Discussion

3.1. Carbon Dioxide Emissions and GWP Analysis

Figure 3 shows the LCA output in terms of global warming potential. In this section, data are reported for each scenario (1 km of road embankment, sections 2 m deep) and the life-cycle stages accounted for in this study. Furthermore, all the processes (production, transportation, and construction) that contribute towards global warming are aggregated in "Cradle to Gate" values.

As can be seen in Figure 3, the production of materials is the phase that contributes to a significant share of the total environmental impact. More specifically, the contribution of production-related impacts ranges between a minimum of 93–94% (for Scenario B | LS and Scenario A | LS, respectively), and a maximum of 96–97% (for Scenario B | QS and Scenario A | QS, respectively). However, it can be noted that the lowest production-related emissions can be recorded for the scenarios involving lignin treatment for the stabilization of the embankment body. This result translates into a lower GWP, considering the cradle-to-gate system. Overall, the contribution of the construction operations is less than 2% of the whole lifecycle. Comparing the two different stabilization techniques (Scenario A | LS vs. Scenario A | QS and Scenario B | LS vs. Scenario B | QS) the results suggest that, for the specific case study, the impacts from transportation and construction activities are approximately comparable.

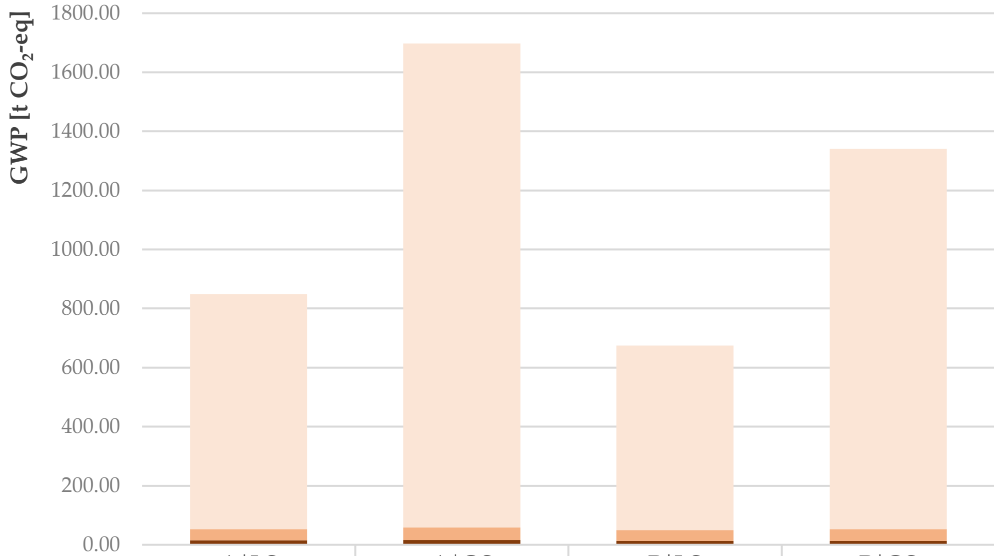

	A∣LS	A∣QS	B∣LS	B∣QS
Production	794.40	1639.05	625.31	1287.52
Transportation	38.04	42.00	37.21	40.48
Construction	15.58	16.09	12.53	12.98
Cradle to Gate	848.02	1697.14	675.05	1340.98

Figure 3. Contribution of each Life-cycle process to Global Warming Potential (GWP).

Figure 4 allows one to quantify the contribution that the production of each input material has to the production of the assessed impact. The production phase was disaggregated to assess the magnitude of each material in terms of GWP.

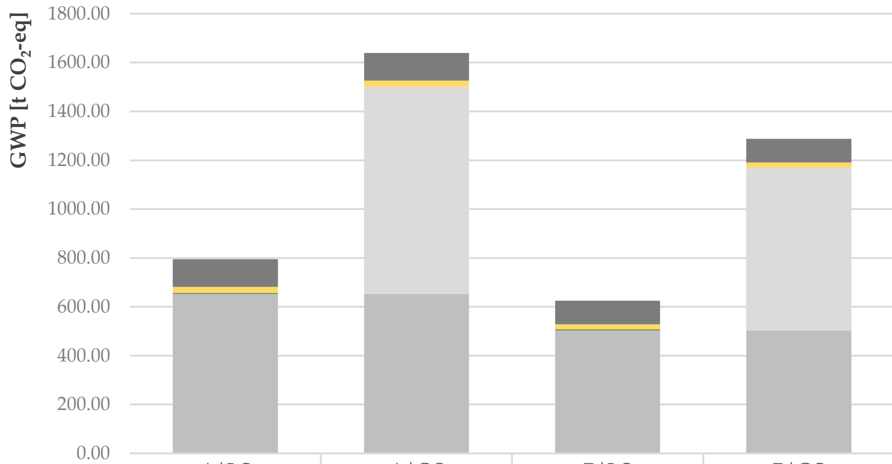

	A∣LS	A∣QS	B∣LS	B∣QS
Aggregates for the coarse-grained layer	112.99	112.99	96.69	96.69
Geotextiles	24.52	24.52	21.07	21.07
Lignin (Embankment body)	4.04		4.15	
Lime (Embankment body)		848.70		666.36
Lime (Subgrade)	652.84	652.84	503.40	503.40

Figure 4. Contribution of the production process of each material to Global Warming Potential (GWP).

Comparing the values for each scenario, the highest rates of GWP are observed for the lime production process. As was expected from the production processes analysis (Section 2.4), lime production generates significant quantities of air pollutants. The environmental impacts of lime production depend largely on limestone decomposition (about 60%), fuel combustion (39%), and electricity consumption (1%) [48].

It is worth noting that lignin is a waste material, and impacts related to its production process are approximately four times lower than the ones obtained for lime.

This analysis does not allow us to draw concrete conclusions about the comparison between the scenarios, as different embankment sizes are taken into account. For this reason, in the following section, the environmental impacts will be compared with each other, referring to a unit of service.

3.2. Carbon Dioxide Emissions and GWP Analysis Per Functional Unit

In this section, to compare the environmental impact of the two stabilization procedures, an analysis was carried out; this referred to the functional unit, which is 1 m^3 (one meter of thickness) of the road embankment section.

GWP and carbon dioxide emissions, generated from construction activities, are reported in Tables 19–21. Information is reported for each sub-process and per functional unit. More specifically, Table 19 summarizes the data for processes that are common to all scenarios. Table 20 shows emissions related to the construction of the embankment body and lignin treatment stabilization. Emissions generated for the construction of the embankment body, involving the lime treatment, are reported in Table 21. This last table includes CO_2 and CO_2-eq emissions related to subgrade construction. It is necessary to underline that, in Tables 20 and 21, two different emission values are reported for the process related to water transportation to the construction site; this is due to the fact that the optimum moisture content is different for Scenario A and Scenario B (thus, the water content per m^3 is different between Scenario A and Scenario B). Tables 19–21 provide the framework for the assessment of emissions generated for various construction operations.

Table 19. CO_2 and CO_2-eq generated for the construction activities common to all scenarios (data Per FU).

Process	Process Code	Applications	CO_2 [kg]	CO_2-eq [kg]
Cleaning and removing topsoil	$E_BT \mid C$	A ǀ LS; A ǀ QS; B ǀ LS; B ǀ QS	0.251	0.258
Excavation for the anti-capillary layer	$E_BT \mid E$	A ǀ LS; A ǀ QS; B ǀ LS; B ǀ QS	0.198	0.203
Transport of the excavated soil to the temporary storage site	$E_BT \mid T$	A ǀ LS; A ǀ QS; B ǀ LS; B ǀ QS	0.111	0.114
Transport of aggregates to the construction site	$A_LC \mid T_a$	A ǀ LS; A ǀ QS; B ǀ LS; B ǀ QS	1.686	1.735
Transport of water to the construction site	$A_LC \mid T_w$	A ǀ LS; A ǀ QS; B ǀ LS; B ǀ QS	0.284	0.292
Compaction of the anti-capillary layer	$A_LC \mid C$	A ǀ LS; A ǀ QS; B ǀ LS; B ǀ QS	0.147	0.151
Geotextiles transport to the construction site	$G_{TX}I \mid T$	A ǀ LS; A ǀ QS; B ǀ LS; B ǀ QS	0.004	0.246
Geotextiles handling and installation	$G_{TX}I \mid L$	A ǀ LS; A ǀ QS; B ǀ LS; B ǀ QS	0.002	0.002
Transport of the A-6 soil	$EC_{LS} \mid T_s$ $EC_{QS} \mid T_s$ $S_{UB}C \mid T_s$	A ǀ LS; A ǀ QS; B ǀ LS; B ǀ QS	0.111	0.114
Precision-finishing	$S_{UB}C \mid F$	A ǀ LS; A ǀ QS; B ǀ LS; B ǀ QS	0.044	0.045

Table 20. CO_2 and CO_2-eq emissions related to lignin-treatment stabilization activities (data per FU).

Process	Process Code	Applications	CO_2 [kg]	CO_2-eq [kg]
Transport of lignin to the construction site	$EC_{LS} \mid T_L$	A ǀ LS; B ǀ LS	0.005	0.006
Transport of water to the construction site	$EC_{LS} \mid T_w$	A ǀ LS B ǀ LS	0.233 0.397	0.239 0.409
Spreading and mixing	$EC_{LS} \mid SM$	A ǀ LS; B ǀ LS	0.260	0.267
Compaction of the layer	$EC_{LS} \mid C$	A ǀ LS; B ǀ LS A ǀ LS; B ǀ LS	0.035 0.020	0.036 0.020

Table 21. CO_2 and CO_2-eq emissions related to lime-treatment stabilization activities (data per FU).

Process	Process Code	Applications	CO_2 [kg]	CO_2-eq [kg]
Transport of lime to the construction site	EC_{QS} ǀ T_Q $S_{UB}C$ ǀ T_Q	A ǀ LS; A ǀ QS; B ǀ LS; B ǀ QS	0.109	0.112
Transport of water to the construction site	EC_{QS} ǀ T_w	A ǀ QS; A ǀ LS	0.306	0.315
	$S_{UB}C$ ǀ T_w	B ǀ QS; B ǀ LS	0.494	0.508
Lime spreading	EC_{QS} ǀ S $S_{UB}C$ ǀ S	A ǀ LS; A ǀ QS; B ǀ LS; B ǀ QS	0.035	0.036
Mixing	EC_{QS} ǀ M $S_{UB}C$ ǀ M	A ǀ LS; A ǀ QS; B ǀ LS; B ǀ QS	0.260	0.267
Compaction of the layer	EC_{QS} ǀ C	A ǀ QS; A ǀ LS	0.030	0.031
	$S_{UB}C$ ǀ C	B ǀ QS; B ǀ LS	0.015	0.015

The most impactful sub-processes are the transport of aggregates to the construction site and the transport of water to achieve the optimum moisture content during embankment construction (both lignin and lime treatments).

Geotextile handling and installation, and the transport of lignin to the construction site, allow us to record the lowest GWP.

Considering the embankment body construction activity, the comparative analysis between the emissions related to lime stabilization and lignin stabilization allows this study to draw the following main conclusions:

i. The difference between emissions generated for the transportation of lignin and lime is significant. From the comparison between the vehicles used in this process (tanker truck for lignin transportation and truck 32 t for lime transportation), it can be noted that the capacity of the truck is approximately twice the capacity of the tanker; furthermore, fuel consumption per km is similar and the distance travelled is the same in both cases. However, the amount of lignin is significantly lower than the required quantity of lime (0.40% vs. 2.5%); as a result, lime transportation generates impacts approximately 20 times higher than lignin transportation.
ii. Emissions from the transportation of water from the source to the site were relatively high, particularly for the lime-treated embankment, as the optimum water content is higher in this scenario compared with the alternative scenario involving lignin stabilization (11.69% vs. 10.33% for the highway and 15.20% vs. 13.40% for the rural road). Furthermore, the optimum moisture content is lower in Scenario A; thus, impacts related to water transportation are significantly reduced for the highway embankment construction.
iii. As reported in Section 2.5.4, the soil stabilizer machine allows to concentrate spreading and mixing in a single process (EC_{LS} ǀ SM). This condition translates into the reduction of fuel consumption and GWP. Compared to the lime-treated embankment scenario, the lignin treatment solution allows us to obtain an approximately 12% decrease in the average values of air pollutants generated during the spreading and mixing of the stabilizing agent with soil.
iv. The compaction effort required in lignin stabilization is higher than the one required in lime soil treatment; thus, the highest number of roller passes is recorded for the lignin-stabilized soil layer (seven vs. six for the highway and four vs. three for the rural road). For this reason, GHGs emissions are slightly higher for A ǀ LS and B ǀ LS scenarios when compared with A ǀ QS and B ǀ QS scenarios, with a percentage increase of about 16%.
v. Overall, the results suggest that scenarios that include lime stabilization in the embankment body construction, allow us to record the highest rates of GWP, both for transportation (includes transportation of A-6 soil, lignin, and water to the construction area) and construction activities (includes soil stabilizer spreading, mixing with existing soil, and compaction operations). In particular, the percentage increase ranges between 51% (Scenario A ǀ QS vs. Scenario A ǀ LS) and 39% (Scenario B ǀ QS vs. Scenario B ǀ LS) for

transportation activities, and between 10% (Scenario A | QS vs. Scenario A | LS) and 11% (Scenario B | QS vs. Scenario B | LS) for construction activities.

4. Conclusions

The Life Cycle Assessment (LCA) is a project-level tool that allows us to assess the environmental impacts of an infrastructure, from raw material production to the end of life phase. In this study, the environmental impacts related to an embankment construction project are investigated by a cradle-to-gate approach. The analysis focuses on all the processes involved in the construction of an embankment section from the base to the preparation of the pavement formation level. Results are provided for two different roads, a highway and a rural secondary road, given the fact that standards require specified structural quality criteria (different for each road type) for the subgrade and embankment layers. Furthermore, two different stabilization methods were investigated including the use of lignin and lime. Stabilization allows us to minimize the environmental impacts, using locally available soil deposits, such as the soil volume, obtained from the excavation of cut sections within the site. All processes that contribute towards global warming are investigated and described in detail. The LCA output, in terms of global warming potential, shows that the production of materials is the phase that contributes a significant share of total environmental impact (more than 90%) for all the scenarios. The lowest production-related emissions can be recorded for the scenarios involving lignin treatment for the stabilization of the embankment body. Moreover, it can be noted that lignin is a waste material and impacts related to its production process are approximately four times lower than the ones obtained for lime. For comparison purposes, the analysis was carried out referring to a functional unit, which is 1 m^3 of the road embankment section. The most important finding of the comparative analysis, between the emissions related to lime stabilization treatment and lignin stabilization treatment of soils, suggests that including lime stabilization in the construction of the embankment body allows us to record the highest rates of GWP, both for transportation and construction activities. The study carried out in this paper provides preliminary results, since calculations were based on several hypotheses, and estimates were made using average values and calculations. For this reason, in future research, attention will be focused on the possibility of overcoming this limit by monitoring the production and construction processes, in order to obtain a more reliable and complete inventory database.

Author Contributions: Conceptualization, G.P. and R.V.; methodology, G.P. and R.V.; investigation, G.P.; data curation, G.P.; writing—original draft, G.P. and M.D.R.; writing—review & editing, G.P., M.D.R., J.D. and R.V.; Supervision, R.V. All authors have read and agreed to the published version of the manuscript.

Funding: This research received no external funding.

Institutional Review Board Statement: Not applicable.

Informed Consent Statement: Not applicable.

Data Availability Statement: Not applicable.

Acknowledgments: The activities of this study are part of the PRIN2017 project "Urban safety, sustainability, and resilience: three paving solutions, four sets of modules, two platforms", acronym: USR342 (prot. 2017XYM8KC), which is gratefully acknowledged.

Conflicts of Interest: The authors declare no conflict of interest.

References

1. Perri, G.; Vaiana, R. Road Safety Management of Uncontrolled Access Points: Design Criteria and Insights into Risk Factors. *Appl. Sci.* **2022**, *12*, 12661. [CrossRef]
2. Special Report 09/2020: The EU Core Road Network. Available online: https://Www.Eca.Europa.Eu/Lists/ECADocuments/SR20_09/SR_Road_network_EN.Pdf (accessed on 19 October 2022).

3. Mantalovas, K.; di Mino, G.; del Barco Carrion, A.J.; Keijzer, E.; Kalman, B.; Parry, T.; Presti, D. lo European National Road Authorities and Circular Economy: An Insight into Their Approaches. *Sustainability* **2020**, *12*, 7160. [CrossRef]
4. Vaiana, R.; Praticò, F. Pavement Surface Properties and Their Impact on Performance-Related Pay Adjustments. In Proceedings of the 3rd International Conference on Transportation Infrastructure, Pisa, Italy, 22–25 April 2014; pp. 22–25.
5. Gulotta, T.; Mistretta, M.; Praticò, F. Life Cycle Assessment of Roads: Material and Process Related Energy Savings. *Model. Meas. Control. C* **2018**, *79*, 146–153. [CrossRef]
6. Garbarino, E.; Quintero, R.R.; Donatello, S.; Wolf, O. *Revision of Green Public Procurement Criteria for Road Design, Construction and Maintenance: Procurement Practice Guidance Document*; Publications Office European Union: Brussels, Belgium, 2016. [CrossRef]
7. European Commission. The European Green Deal. COM (2019) 640 Final. Available online: https://Eur-Lex.Europa.Eu/Resource.Html?Uri=cellar:B828d165-1c22-11ea-8c1f-01aa75ed71a1.0002.02/DOC_2&format=PDF (accessed on 10 November 2022).
8. Araújo, J.P.C.; Oliveira, J.R.M.; Silva, H.M.R.D. The Importance of the Use Phase on the LCA of Environmentally Friendly Solutions for Asphalt Road Pavements. *Transp. Res. Part D Transp. Environ.* **2014**, *32*, 97–110. [CrossRef]
9. Lettner, M.; Solt, P.; Rößiger, B.; Pufky-Heinrich, D.; Jääskeläinen, A.S.; Schwarzbauer, P.; Hesser, F. From Wood to Resin—Identifying Sustainability Levers through Hotspotting Lignin Valorisation Pathways. *Sustainability* **2018**, *10*, 2745. [CrossRef]
10. Azarijafari, H.; Yahia, A.; ben Amor, M. Life Cycle Assessment of Pavements: Reviewing Research Challenges and Opportunities. *J. Clean. Prod.* **2016**, *112*, 2187–2197. [CrossRef]
11. Praticò, F.G.; Giunta, M.; Mistretta, M.; Gulotta, T.M. Energy and Environmental Life Cycle Assessment of Sustainable Pavement Materials and Technologies for Urban Roads. *Sustainability* **2020**, *12*, 704. [CrossRef]
12. Gulotta, T.M.; Mistretta, M.; Praticò, F.G. A Life Cycle Scenario Analysis of Different Pavement Technologies for Urban Roads. *Sci. Total Environ.* **2019**, *673*, 585–593. [CrossRef]
13. Praticò, F.G.; Vaiana, R.; Giunta, M.; Iuele, T.; Moro, A. Recycling PEMs Back to TLPAs: Is That Possible Notwithstanding RAP Variability? *Appl. Mech. Mater.* **2013**, *253–255*, 376–384. [CrossRef]
14. Ciampa, D.; Cioffi, R.; Colangelo, F.; Diomedi, M.; Farina, I.; Olita, S. Use of Unbound Materials for Sustainable Road Infrastructures. *Appl. Sci.* **2020**, *10*, 3465. [CrossRef]
15. Praticò, F.; Saride, S.; Puppala, A. Comprehensive Life-Cycle Cost Analysis for Selection of Stabilization Alternatives for Better Performance of Low-Volume Roads. *Transp. Res. Rec. J. Transp. Res. Board* **2011**, *2204*, 120–129. [CrossRef]
16. Celauro, C.; Corriere, F.; Guerrieri, M.; lo Casto, B.; Rizzo, A. Environmental Analysis of Different Construction Techniques and Maintenance Activities for a Typical Local Road. *J. Clean. Prod.* **2017**, *142*, 3482–3489. [CrossRef]
17. Vaiana, R.; Iuele, T.; Gallelli, V.; Tighe, S.L. Warm Mix Asphalt by Water-Containing Methodology: A Laboratory Study on Workability Properties versus Micro-Foaming Time. *Can. J. Civ. Eng.* **2013**, *41*, 183–190. [CrossRef]
18. Huang, Y.; Bird, R.; Heidrich, O. Development of a Life Cycle Assessment Tool for Construction and Maintenance of Asphalt Pavements. *J. Clean. Prod.* **2009**, *17*, 283–296. [CrossRef]
19. Hermansson, F.; Janssen, M.; Svanström, M. Correction to: Allocation in Life Cycle Assessment of Lignin. *Int. J. Life Cycle Assess.* **2020**, *25*, 2099–2100. [CrossRef]
20. Zhang, T.; Cai, G.; Liu, S. Application of Lignin-Based by-Product Stabilized Silty Soil in Highway Subgrade: A Field Investigation. *J. Clean. Prod.* **2017**, *142*, 4243–4257. [CrossRef]
21. Bajwa, D.S.; Pourhashem, G.; Ullah, A.H.; Bajwa, S.G. A Concise Review of Current Lignin Production, Applications, Products and Their Environmental Impact. *Ind. Crop. Prod.* **2019**, *139*, 111526. [CrossRef]
22. Pérez, I.P.; Rodríguez Pasandín, A.M.; Pais, J.C.; Alves Pereira, P.A. Use of Lignin Biopolymer from Industrial Waste as Bitumen Extender for Asphalt Mixtures. *J. Clean. Prod.* **2019**, *220*, 87–98. [CrossRef]
23. Gaudenzi, E.; Cardone, F.; Lu, X.; Canestrari, F. Analysis of Fatigue and Healing Properties of Conventional Bitumen and Bio-Binder for Road Pavements. *Materials* **2020**, *13*, 420. [CrossRef]
24. Abdelsalam, M.; Yue, Y.; Khater, A.; Luo, D.; Musanyufu, J.; Qin, X. Laboratory Study on the Performance of Asphalt Mixes Modified with a Novel Composite of Diatomite Powder and Lignin Fiber. *Appl. Sci.* **2020**, *10*, 5517. [CrossRef]
25. Vaiana, R.; Oliviero Rossi, C.; Perri, G. An Eco-Sustainable Stabilization of Clayey Road Subgrades by Lignin Treatment: An Overview and a Comparative Experimental Investigation. *Appl. Sci.* **2021**, *11*, 11720. [CrossRef]
26. Zhang, T.; Cai, G.; Liu, S. Application of Lignin-Stabilized Silty Soil in Highway Subgrade: A Macroscale Laboratory Study. *J. Mater. Civ. Eng.* **2018**, *30*, 04018034. [CrossRef]
27. Ministero delle Infrastrutture e dei Trasporti. Decreto Ministeriale n.6792 del 05/11/2001. Norme Funzionali e Geometriche per la Costruzione delle Strade. In *Gazzetta Ufficiale della Repubblica Italiana*; Ministero delle Infrastrutture e dei Trasporti: Roma, Italy, 2001.
28. Bheemasetti, T.V.; Pedarla, A.; Puppala, A.J.; Acharya, R. Design of Sustainable High-Volume Pavements Using Controlled Low-Strength Material from Native Soil. *Transp. Res. Rec. J. Transp. Res. Board* **2015**, *2509*, 10–17. [CrossRef]
29. Okyay, U.S.; Dias, D. Use of Lime and Cement Treated Soils as Pile Supported Load Transfer Platform. *Eng. Geol.* **2010**, *114*, 34–44. [CrossRef]
30. Ardah, A.; Chen, Q.; Abu-Farsakh, M. Evaluating the Performance of Very Weak Subgrade Soils Treated/Stabilized with Cementitious Materials for Sustainable Pavements. *Transp. Geotech.* **2017**, *11*, 107–119. [CrossRef]
31. Ministero dei lavori pubblici. Centro Sperimentale Interuniversitario Di Ricerca Stradale (CIRS). In *Capitolato Speciale d'appalto Tipo per Lavori Stradali*; Ministero dei lavori pubblici: Roma, Italy, 2001.

32. Harvey, J.; Kendall, A.; Lee, I.-S.; Santero, N.; van Dam, T.; Wang, T. Pavement Life Cycle Assessment Workshop: Discussion Summary and Guidelines. Available online: https://Escholarship.Org/Uc/Item/3jc3d3xs (accessed on 20 October 2022).
33. Emission Factors for Greenhouse Gas Inventories. Available online: https://www.Epa.Gov/Sites/Default/Files/2015-07/Documents/Emission-Factors_2014.Pdf (accessed on 8 October 2022).
34. Barbieri, D.M.; Lou, B.; Wang, F.; Hoff, I.; Wu, S.; Li, J.; Vignisdottir, H.R.; Bohne, R.A.; Anastasio, S.; Kristensen, T. Assessment of Carbon Dioxide Emissions during Production, Construction and Use Stages of Asphalt Pavements. *Transp. Res. Interdiscip. Perspect.* **2021**, *11*, 100436. [CrossRef]
35. United States Environmental Protection Agency (EPA). *Emission Factors for Greenhouse Gas Inventories*; United States Environmental Protection Agency (EPA): Washington, DC, USA, 2022.
36. Stripple, H. *Life Cycle Assessment of Road: A Pilot Study for Inventory Analysis*, 2nd ed.; IVL RAPPORT; Swedish National Road and Transport Research Institute (VTI): Stockholm, Sweden, 2001.
37. Trani, M.L.; Bossi, B.; Gangolells, M.; Casals, M. Predicting Fuel Energy Consumption during Earthworks. *J. Clean. Prod.* **2016**, *112*, 3798–3809. [CrossRef]
38. Cabello Eras, J.J.; Gutiérrez, A.S.; Capote, D.H.; Hens, L.; Vandecasteele, C. Improving the Environmental Performance of an Earthwork Project Using Cleaner Production Strategies. *J. Clean. Prod.* **2013**, *47*, 368–376. [CrossRef]
39. Aurangzeb, Q.; Al-Qadi, I.L.; Ozer, H.; Yang, R. Hybrid Life Cycle Assessment for Asphalt Mixtures with High RAP Content. *Resour. Conserv. Recycl.* **2014**, *83*, 77–86. [CrossRef]
40. Directorate General Joint Research Centre (JRC). European Reference Life Cycle Database (ELCD); European Commission. Available online: https://eplca.jrc.ec.europa.eu/ELCD3/ (accessed on 11 October 2022).
41. Kecojevic, V.; Komljenovic, D. Impact of Bulldozer's Engine Load Factor on Fuel Consumption, CO_2 Emission and Cost. *Am. J. Environ. Sci.* **2011**, *7*, 125–131. [CrossRef]
42. Celauro, C.; Corriere, F.; Guerrieri, M.; lo Casto, B. Environmentally Appraising Different Pavement and Construction Scenarios: A Comparative Analysis for a Typical Local Road. *Transp. Res. Part D Transp. Environ.* **2015**, *34*, 41–51. [CrossRef]
43. Serafini, F. *Il Manuale per La Progettazione e Costruzione Delle Strade*; Geo-Graph: Milan, Italy, 1994.
44. Caterpillar Tractor Company. *Caterpillar Performance Handbook*, 49th ed.; Caterpillar Tractor Company: Peoria, IL, USA, 2019.
45. Niphadkar, N. Relationship between Number of Passes of Compactor and Compaction Characteristics of Soil. *Intern. Res. J. Eng. Tech.* **2016**, *3*, 728–732.
46. National Stone Sand & Gravel Association the Aggregates Industry Greenhouse Gases: Low Emissions, High Resiliency. Available online: https://Www.Nssga.Org/Sites/Default/Files/2021-05/NSSGAGreenhouseGasEmissionsReport04-26-21.Pdf (accessed on 11 September 2022).
47. Raja, J.; Dixon, N.; Fowmes, G.; Frost, M.; Assinder, P. Obtaining Reliable Embodied Carbon Values for Geosynthetics. *Geosynth. Int.* **2015**, *22*, 393–401. [CrossRef]
48. Laveglia, A.; Sambataro, L.; Ukrainczyk, N.; de Belie, N.; Koenders, E. Hydrated Lime Life-Cycle Assessment: Current and Future Scenarios in Four EU Countries. *J. Clean. Prod.* **2022**, *369*, 133224. [CrossRef]
49. Modahl, I.S.; Soldal, E. The 2019 LCA of Products from Borregaard, Sarpsborg; Report No. OR.14.21 Open Version. 2021. Available online: https://norsus.no/wp-content/uploads/OR.14.21-Open-The-2019-LCA-of-products-from-Borregaard-Sarpsborg-.pdf?v=1 (accessed on 12 September 2022).
50. AASHTO. *Standard Specification for Classification of Soils and Soil–Aggregate Mixtures for Highway Construction Purposes*; AASHTO M145-91 (2008); AASHTO: Washington, DC, USA, 2008.
51. Müller, W.W.; Saathoff, F. Geosynthetics in Geoenvironmental Engineering. *Sci. Technol. Adv. Mater.* **2015**, *16*, 034605. [CrossRef] [PubMed]
52. Fuc, P.; Kurczewski, P.; Lewandowska, A.; Nowak, E.; Selech, J.; Ziolkowski, A. An Environmental Life Cycle Assessment of Forklift Operation: A Well-to-Wheel Analysis. *Int. J. Life Cycle Assess.* **2016**, *21*, 1438–1451. [CrossRef]